

1 **Soil contamination by microplastics in relation to local agricultural** 2 **development as revealed by FTIR, ICP-MS and pyrolysis-GC/MS**

3

4 Khawla Chouchene^{1*}, Tommaso Nacci ², Francesca Modugno^{2,3}, Valter Castelvetro^{2,3} and
5 Mohamed Ksibi^{1,4}

6 1) Laboratory of Environmental Engineering and Ecotechnology (LGEET-ENIS), University of Sfax, Tunisia

7 2) Department of Chemistry and Industrial Chemistry, University of Pisa, Pisa (Italy)

8 3) CISUP—Center for the Integration of Scientific Instruments of the University of Pisa, Pisa, Italy

9 4) Higher Institute of Biotechnology of Sfax (ISBS), University of Sfax, Tunisia

10 * corresponding authors: chouchene.khawla23@gmail.com

11 **Abstract**

12 Plastic film mulching and use of wastewaters for irrigation have been common
13 agricultural practices for over half a century in Tunisia, especially in arid regions,
14 resulting in the undesired creation of a pathway for microplastics (MPs) to enter
15 farmland soil. In order to assess the extent and characteristics of soil contamination by
16 MPs in the Moknine province, an area of intensive agricultural practices, 16 farmland
17 soil samples were collected and characterized. The total concentration of targeted MPs
18 was 50-880 items/kg; among them, the most common MPs type being polypropylene
19 (PP), mainly occurring as white/transparent fibers with small size (cross section <0.3
20 mm). SEM images of MPs surfaces revealed multiple features related to environmental
21 exposure and degradation. ATR-FTIR spectroscopy and pyrolysis-GC/MS analyses
22 enabled the accurate identification of MPs separated from the embedding soil micro-
23 and macro-aggregates. Finally, contamination of the polymeric microparticles with a
24 broad range of metals was found by ICP-MS analysis, suggesting that MPs can be
25 vectors for transporting heavy metals in the soil and indicators of soil contamination as
26 a result of mismanagement of industrial wastewaters.

27 **Key words**

28 Polymer microparticles, Intensive agriculture, Pyrolysis-Gas Chromatography-Mass
29 Spectrometry, Infrared spectroscopy, Heavy metals, Moknine province.

30 **1. Introduction**

31 Recent research has been focused on assessing the main sources of MPs and their
32 environmental distribution as a prerequisite to evaluate how they affect the
33 contaminated biosphere (Pinto, 2018). Two broad categories can be distinguished as the
34 sources of MPs; primary particles fabricated as such are present as micro- or nano-beads
35 in personal care and industrial product formulations, while secondary particles result
36 from the constant weathering and abrasion or fragmentation of plastic items occurring
37 upon dispersion in the environment (Chouchene et al., 2019). Waste mismanagement
38 and uncontrolled dumping results in an increasing amount of plastics accumulating in
39 terrestrial as well as aquatic environments (Samir et al., 2021), also due to the very slow
40 degradation of synthetic polymers under normal photo-oxidative and hydrolytic
41 conditions. MPs can also behave as collectors and concentrators of toxic environmental
42 pollutants (Chouchene et al., 2020). While MPs are increasingly recognized as a serious
43 threat for natural aquatic environments, it is inland where most of the plastic items are
44 produced, used, and disposed of. Uncontrolled disposal and subsequent environmental
45 (mainly photo-oxidative) polymer degradation may thus result in a significant inflow of
46 MPs also in terrestrial environments, where they may accumulate in soils before
47 reaching the groundwater table and eventually riverine and marine ecosystems (Afrin et
48 al., 2020; Steinmetz et al., 2016). Studies support the alarm about using wastewater
49 treatment plants (WWTP) sludges as fertilizers and urban or industrial wastewaters for
50 agricultural land irrigation, both practices being important sources for soil
51 contamination by MPs (Nizzetto et al., 2016). Indeed, WWTP and sewage sludges have
52 been identified as the receptors of MPs including a significant fraction of synthetic
53 fibers (Corradini et al., 2019). Additional sources of MPs in agricultural soils are plastic
54 mulch films (mainly polyethylene, PE, and its copolymers with vinyl alcohol or butyl
55 acrylate) and other plastic items (greenhouse covers, strings and nets supporting
56 growing plants, etc.) widely used in intensive farming.

57 More than 700.000 ton of MPs are estimated to enter the soil annually in North America
58 and Europe, a quantity larger than the 93.000-236.000 ton of MPs estimated to be
59 floating in oceanic surface waters (Van Sebille et al., 2015). Increasing evidences
60 indicate some MPs toxicity for organisms that are important indicators of a healthy
61 agricultural soil, as in the studies concerning the oligochaeta *Enchytraeus crypticus* and
62 *Lumbricus terrestris* (earthworm) exposed to soils containing 10 wt% polystyrene (PS)
63 (Zhu et al., 2018) and 28-60% PE (Lwanga et al., 2016) MPs, respectively. MPs have

64 the ability to convey toxic pollutants with endocrine disrupting ability within soil-plant
65 system, whether by adsorption of toxic chemicals from their polluted environment, or
66 from their own suite of potentially toxic additives (Zhu et al., 2018). Nevertheless, the
67 contribution of the internal sources (i.e., plastics in agricultural practice) on the
68 occurrence of MPs in is not well-known.

69 In the case of Tunisia, the limited experimental research on plastics pollution has
70 focused until now on macroplastics. The Moknine province, located in the center-east of
71 Tunisia, is a typical agricultural area characterized by intensive use of plastics mulches
72 and extensive greenhouse coverage (43.5% of the total area of the greenhouses in
73 Tunisia) for growing vegetables and fruits; thus the soil health in this area is of utmost
74 importance. Farmers in Moknine have been using plastic film for mulching and
75 greenhouse for quite a long time due to its convenience and cheap price. In this work,
76 the concentration of MPs in a representative agricultural land of the Moknine province
77 was assessed, distinguished by polymer types. This was intended as a first step to
78 increase the knowledge on the MPs sources and accumulation in the agricultural soil,
79 thereby providing scientific background to the setting up a management plan including
80 reduction or redesign of the use of plastic in this ecosystem. In detail, the objectives of
81 this study are: 1) to assess the abundance of MPs contamination in intensive agriculture
82 soils; 2) to assess the characteristics and spatial distribution of MPs in a typical city
83 suburban area; 3) to evaluate the efficacy and accuracy of Py-GC/MS and DSC methods
84 as compared to the most common FTIR analysis for the identification of polymers in
85 MPs.

86

87 **2. Materials and methods**

88 *2.1. Description of the study site*

89 Moknine city is situated in the middle of eastern Tunisia (35°37'–35°35'E and 10°55'–
90 10°53'N), in an area separated from the Mediterranean Sea by a 4–6 km wide littoral
91 barrier. In spite of being a small province, with an estimated population of 75.885,
92 Moknine was selected to run this study because of the record application in agriculture
93 of sludge, mulching and greenhouse covers for many years now. Moknine city has been
94 connected to a wastewater treatment plant (WWTP) since 1983.

95 *2.2. Sampling procedure*

96 Agricultural soil samples from 16 points were collected as the top 20 cm using a soil
97 hand auger (Fig.1). About 1 kg of soil was sampled at each point and placed into an
98 aluminum bag, then the samples were transported to the laboratory and stored at 4 °C
99 before treatment. Before the analyses, each soil sample was homogenized by
100 mechanical mixing, then dried in an oven at 40 °C. Once dried the soil formed hard
101 clods, therefore the samples were mildly hand-milled in a porcelain mortar and sieved
102 through a cascade of 5, 2-, 1-, 0.5-, and 0.3-mm mesh size stainless-steel sieves, giving
103 five size classes (<0.3, 0.3-0.5, 0.5-1, 1-2 and 2-5mm), prior to the extraction procedure.
104 When present, visually detectable plastic particles were separated with tweezers and
105 counted by hand.

106 *2.3. Microplastic extraction and purification*

107 MPs extraction was performed according to a previously described procedure
108 (Chouchene et al., 2020, 2019). 200 g of dried sample for each one of the smaller sized
109 classes (<0.3, 0.3-0.5, 0.5-1 mm) was suspended in aqueous 1.2 g/L NaCl solution in a
110 1 L glass beaker. The mixture was thoroughly manually stirred for 15 min, then allowed
111 to stand for 30 min to allow density separation by flotation of the less dense MPs. The
112 supernatant was filtered through paper filter (Prat-Dumas flat filter diam. 7-9 µm;
113 QNDM-090-100), then the filter with the MPs debris was placed in a culture dish and
114 digested with aqueous 10 % KOH solution to remove the organic matter soiling the
115 MPs. Flotation and filtration steps were repeated until no more floating particles could
116 be detected and recovered, with a minimum of 3 repetitions. The collected particles
117 were inspected at 10×magnification using a Realux CFM-7045 B2 stereomicroscope
118 (COFEMO, France), and sorted according to their shapes: fragment, fibers, granules,
119 tubes, and foams, respectively. In addition, each isolated particle was classified and
120 numbered by color and size.

121 *2.4. Analytical techniques*

122 Fourier-transform infrared spectroscopy (FTIR) analysis for the identification of the
123 polymers extracted as MPs from the soil samples was performed using a Perkin Elmer
124 Spectrum BX Fourier transformed infrared spectrometer operating in transmission mode
125 (64 scans, 4 cm⁻¹ resolution, spectral range 4000–650 cm⁻¹).

126 A model STA 409PC Differential Scanning Calorimeter (Netzsch, Germany) equipped
127 with a Pt/Rh crucible with lid was used for DSC analysis. The sample was heated from

128 20-800 °C at 5 K·min⁻¹ under nitrogen atmosphere (purge: 50 mL/min; protective: 20
129 mL/min) to suppress oxidation. An empty Pt/Rh crucible served as reference.
130 Integration of the DSC peaks was realized using the ChemStation Software
131 (Ver.A09.01) from Agilent Technologies.

132 The Pyrolysis-GC/MS instrumentation consisted of a Multi-Shot Pyrolyzer EGA/Py-
133 3030D micro-furnace (Frontier Laboratories Ltd., Fukushima, JP) coupled to a 8890
134 Gas Chromatograph (GC, Agilent Technologies, Palo Alto, USA) that was equipped
135 with a deactivated silica pre-column (2 m x 0.32 mm i.d., Agilent J&W, USA) and an
136 HP-5MS fused silica capillary column (stationary phase 5 % diphenyl - 95% dimethyl-
137 polysiloxane, 30 m x 0.25 mm i.d., 0.25 µm, Hewlett Packard, USA). Ten fibers, each
138 one characterized by a different color, were selected for Py-GC-MS: four fibers (2-
139 white and 2-blue) from sample 3, three fibers (grey, blue, and white) from sample 6, and
140 three fibers (yellow, green and grey) from sample 11, all of which had previously been
141 identified by FTIR analysis. About 80 µg of each one of the ten selected particles was
142 placed into a clean stainless-steel cup, inserted in the microfurnace with an Auto-Shot
143 sampler AS-1020E (Frontier Laboratories Ltd. Fukushima, JP) and pyrolyzed at 600 °C
144 for 0.20 min. The detector was an Agilent 5977 Mass Selective Detector (Palo Alto,
145 USA) single quadrupole mass spectrometer operating in electron ionization mode (EI)
146 at 70 eV, in positive mode scanning in the range from 35-550 m/z. The MS ion source
147 temperature was 230 °C and the MS quadrupole temperature 150 °C. The injection port
148 was set at 280 °C, with 1:20 split ratio, and the interface temperature was 280 °C. The
149 pyrolysis products were eluted in constant flow mode at 1.0 mL/min (carrier gas He,
150 purity 99.995%) with the following chromatographic program: initial isothermal step at
151 40 °C for 6 min, heating at 20 °C/min to 310 °C, then isothermal step for 40 min. The
152 data collected were processed by MassHunter Workstation (version10.0) and the NIST
153 Mass Spectral Search Program 2.4.

154 Analysis of trace metals as contaminants of MPs was carried out by Inductively
155 Coupled Plasma-Mass Spectrometry (ICP-MS) (Thermo Scientific iCAP7000series).
156 Four representative plastic particles were selected for this purpose from the different
157 sampling sites: a fragment from sample 7, a blue fragment from sample 1, a white fiber
158 from samples 13, and a transparent fragment from sample 15. The fragment from the
159 sample 7 was sonicated in an ultrasonic bath to complete the removal of residual soiling
160 material. The plastic particles were transferred into centrifuge tubes, added with 65 %

161 HNO₃ and then 30 % H₂O₂, and heated for 30 min at 100 °C. Five control blank
162 solutions containing 30 ppm, 10 ppm, 1 ppm, 0.1 ppm, 0.05 ppm, and 0.01 ppm,
163 respectively, of combined Cr, Ag, Cu, Hg, Mn, Fe, Ni, Zn, Ti, As, Co, Al, and Cd
164 standard solution (1000 mg/L in aqueous HNO₃) were prepared to ensure precision and
165 accuracy.

166 Elemental analysis for the metal content of the soil samples was performed with a
167 iCE3000 Series Atomic Absorption Spectrometer (Thermo Scientific, Cambridge, UK).
168 About 1 g of soil was weighed into a PTFE vessel with 1 mL HNO₃ and 3 mL HCl for
169 microwave digestion. All the samples were heated at 10 °C/min to 120 °C, and after 10
170 min digestion at 120 °C and 1000 W were allowed to cool down to room temperature.
171 After cooling, the volume was adjusted until 25 mL with distilled water before
172 performing the analysis.

173 Scanning Electron Microscopy (SEM) analysis was performed on 13 particles
174 representative of all the different polymer types detected in the soil samples (Table S-1
175 in the Supplementary Data, SD). Among them, particles from sample 7 and 2 required
176 additional cleaning before the analysis; thus, they were suspended in deionized water
177 and sonicated in a sonication bath for 15 min at 40 °C to remove residual soiling
178 material. Subsequently, surface topography and roughness of MPs sputter coated with
179 platinum was observed using a scanning electron microscope (SEM Quanta FEG450)
180 operated at 15 kV.

181 *2.5. Quality Assurance and Quality Control*

182 To prevent contamination by airborne MPs, strict quality control was carried out during
183 the experiment. The metal auger was rinsed before and after taking the soil samples. All
184 sieves, tweezers, containers, beakers and equipment were rinsed carefully with distilled
185 water. All culture dishes and suction filters used during the experiment were washed
186 and covered with aluminum foil for each step. Cotton laboratory coats was always worn
187 during the sampling process and lab work. During laboratory work, procedural blanks
188 were run by placing 250 mL of distilled water in the same glass containers used for
189 samples extraction and leaving them uncovered on lab benches during the extraction
190 process. Blank experiments performed in triplicate and run in parallel with the samples
191 in the laboratory did not show any evidence of MPs contamination from the lab
192 environment.

193 3. Results and discussions

194 3.1. Abundance and spatial distributions of MPs

195 In the investigated area of the Moknine province, MPs particles were detected in all
196 samples of agricultural soil collected across the 16 sampling points, at concentrations
197 ranging between 50-880 p·kg⁻¹ with average abundance of 161 p·kg⁻¹. The maximum
198 concentration of MPs was 880 p·kg⁻¹, that is higher than the 593 p·kg⁻¹ reported for
199 samples soils of Swiss floodplains (Scheurer and Bigalke, 2018), and much higher than
200 the 4.5 p·kg⁻¹ found in a Shanghai aquaculture farmland (Lv et al., 2019) and the 78-62
201 p·kg⁻¹ in a farmland in the suburbs of Shanghai (Liu et al., 2018). On the other hand,
202 MPs concentrations found in the present study are lower than those reported for Shaanxi
203 agricultural soils, Hangzhou Bay soils (Ding et al., 2020) and the coastal soil of
204 Shandong province (Zhou et al., 2018). Two kinds of shapes were detected in this study
205 as shown in Fig. 2. The sampling area of the present study is not located in the
206 immediate vicinity of the industrial zone or of densely populated areas, therefore the
207 detected soil pollution by MPs cannot be ascribed to a direct input from wastewaters or
208 from other types of anthropogenic wastes. Results of this study showed that the soil
209 around the olive trees in Moknine province was also polluted with MPs (55-105 p·kg⁻¹),
210 suggesting that these inputs were randomly dumped scraps. Additional sources of
211 pollution by MPs could be fragmentation of weathered plastic items entering the land
212 through littering. Moreover, the comparatively low concentration of 50 p·kg⁻¹ found in
213 the arid land of the sampling site 16 suggests that organic/inorganic matter could
214 facilitate the settlement and the aggregation of MPs (Chairi et al., 2010). The maximum
215 concentration of MPs was found in the soils sampled in areas where greenhouses are
216 more common, suggesting a correlation between such agricultural practices and the
217 accumulation of MPs in the Moknine province.

218 3.2. Shapes, colors and sizes distribution

219 The diversity of MPs characteristics such as size, colors, and shapes were analyzed as
220 they are thought to play a critical role in the translocation within the soil food web.
221 Irregularly shaped fragments and curly fibrous MPs were the most abundant types,
222 accounting for 41 % and 59 % of the total, respectively (Fig.S-1.a), while pellets were
223 the less common particles. A predominant concentration of film fragments and fibers
224 has been reported in several other studies (Ding et al., 2020; Zhou et al., 2018, 2019;

225 Ding et al., 2020; Scheurer and Bigalke, 2018), in which it has also been correlated with
226 intensive use of plastic film, of wastewater for irrigation, and of sewage sludge for
227 agricultural soil amendment. Among the sampling sites explored in this study, common
228 relative number of fibers and fragments have been discovered.

229 The detected MPs were classified into five size ranges, namely <0.3, 0.3-0.5, 0.5-1, 1-2
230 and 2-5 mm (Fig.S-1.b). In all the soil samples, the size <1mm was the most abundant
231 with 74% of the total number of particles. The <0.3 and 0.3-0.5 mm fractions counted
232 for over 20% of the total (Fig.S-1). The higher fraction of smaller sized MPs was again
233 in good agreement with previous results (Chen et al., 2019; Scheurer and Bigalke,
234 2018), and is clearly the result of oxidative degradation caused by the intensive
235 exposure to UV radiation and high temperature (Chai et al., 2020). The number
236 concentration of small sized MPs in the ranges <0.3 and 0.3-0.5 mm reported above, is
237 likely due to the fragmentation of macroscopic plastic items into large MPs and then,
238 with an obvious multiplying factor, into progressively smaller ones, posing specific
239 threats to the terrestrial and nearby aquatic organisms.

240 As shown in Fig.S-1.c, MPs of ten colors were found. Colorless particles were the most
241 abundant (49.1 %), followed by blue (20.3 %), white (18.6 %), green (3.1 %), black (3
242 %), grey and yellow (2.7 %), red and maroon (1.1 %) and less defined colors (1.0 %).
243 Of these, colorless and blue/green were the dominant MPs in the smaller <0.3 and 0.3-
244 0.5 mm classes. Overall, different size classes of MPs tended to have different color
245 distribution. Fragments were predominantly white/transparent and blue/green in color,
246 while fibers were more diverse in color. Soils of greenhouse sample contained mostly
247 white/transparent fragments and blue fibers, probably associated with the improper
248 disposal of plastic sheets and missed collection of mulching plastics, suggesting a close
249 correlation between MPs pollution and degradation of this specific kind of plastic waste
250 that will keep accumulating unless more appropriate agricultural plastic waste
251 management is adopted. However, the light-colored MPs found in this study could also
252 be the result of weathering causing discoloration and fading as mentioned by (Galafassi
253 et al., 2019).

254 3.3. Identification of microplastics extracted from soil samples

255 FTIR results

256 Six different polymer kinds were identified as the constituents of the two types of MPs
257 (fragments and fibers), based on their FTIR spectra: branched, low density polyethylene
258 (LDPE) and linear, high-density polyethylene (HDPE, collectively PE), aliphatic
259 polyamide (nylon, Ny), polypropylene (PP), polyacrylonitrile (PAN), polyester
260 (polyethylene terephthalate, PET), and cellulose (natural or regenerated). Representative
261 transmittance spectra recorded from individual MPs are shown in Fig.S-2.

262 The polymer type for each MP found in the soil samples has been identified based on
263 polymer-specific absorption bands (Table S-2 in the SD). The two different PE types
264 could be distinguished by inspection of the spectral regions between 2950 cm^{-1} and
265 2850 cm^{-1} (C-H stretching bands) and between 1475 cm^{-1} and 1350 cm^{-1} (methylene
266 and methyl deformations): the presence of a shoulder at 2950 cm^{-1} (methyl asymmetric
267 C-H stretching) and the higher relative intensity of the shoulder in the $1400\text{-}1375\text{ cm}^{-1}$
268 range (methyl symmetric bending deformation) compared to the absorption band at
269 about 1460 cm^{-1} (methylene scissoring deformation) are indicative of branched
270 polyolefins such as LDPE. DSC analysis of the two fragments identified by FTIR as PE
271 gave relatively sharp melting transitions peaking at $124\text{ }^{\circ}\text{C}$ (Fig.S-3), which is typical of
272 a highly crystalline LLDPE or of heavily oxidized HDPE (Li et al., 2019) the latter
273 being more likely for highly oxidized particles as detected by FTIR.

274 PP was the dominant polymer in the soil samples, accounting for 50 % of the total
275 number of particles, followed by PE (24 %), and smaller amounts of other polymers
276 such as PAN (9 %), Ny and PET (8 %). The MPs composition was variable with the
277 sampling site, but PE and PP were a common and dominant presence. Fibers typically
278 consisted of PE, PP, PAN, PET, and cellulose. Overall, PP was the dominant fiber type,
279 likely as a result of its use (bags, nets) in the agricultural practice. PAN, PET and Ny
280 fibers, along with cellulosic ones, were mainly attributed to release and dispersion of
281 staple fibers from textiles into laundry wastewaters used for irrigation or contained in
282 wastewater treatment plant sludge used as agricultural soil amendment. Small fragments
283 consisted almost exclusively of PP along with some PE, most likely resulting from the
284 mechanical fragmentation of weathered plastic sheets used for greenhouse, as protecting
285 covers against adverse environmental factors for grapes in vineyards, and as mulching
286 films (LDPE/HDPE) not removed from the farmed land at the end of the useful life
287 cycle. Additional MPs from the above polyolefins may result from the environmental
288 degradation of improperly disposed waste from e.g. pesticides and fertilizers packaging

289 (mainly LDPE and PP), and, to a lesser extent, from water irrigation pipes (HDPE).
290 Indeed, a common feature of all the recorded FTIR spectra, and particularly so for those
291 of fully hydrocarbon backbone polymers (PE, PP, PAN), was the presence of hydroxyl
292 ($3200\text{-}3500\text{ cm}^{-1}$), carbonyl ($1700\text{-}1800\text{ cm}^{-1}$), and various C-O-C and C-O-O (1000-
293 1200 cm^{-1} from ether, ester, alcohol, peroxide groups) absorptions, indicating extensive
294 photo-oxidative degradation due to natural weathering; the resulting polymer
295 embrittlement promotes then their fragmentation into secondary MPs.

296 The presence of all the above polymers as MPs pollutants in agricultural soils, with a
297 significant direct contribution from agricultural activities, has been reported before (Liu
298 et al., 2018; Lv et al., 2019). A peculiarity of the sampled sites in Moknine province is
299 the presence of nearby sabkhas, areas in North Africa coastal flats rich in salts as they
300 are subject to periodic flooding and evaporation. In the specific case of Moknine
301 catchment, the sabkhas suffer from contamination by heavy metals, as a result of
302 industrial activities disposing there about a half of their wastewaters (Wali et al., 2015),
303 and by plastic waste originating from urban settlements. While such polluted sites in the
304 Moknine province have not undergone any environmental remediation treatment,
305 making their soils as likely “hotspots” for pollution by both heavy metals and MPs,
306 they have been, and are still used today, to grow various crops.

307 *Pyrolysis-GC/MS results*

308 Py-GC/MS has been used to identify MPs from different matrices (Primpke et al.,
309 2020). The GC/MS profiles recorded upon pyrolysis at $600\text{ }^{\circ}\text{C}$ of individual sampled
310 particles were compared with data bases from the literature (Orsini et al., 2017); specific
311 polymer markers identified among the pyrolysis products are listed in Table S-3 in the
312 Supplementary Data, while a more exhaustive list of the main pyrolysis products is
313 reported in Table S-4 in the SD. Fibers of animal origin were identified by the presence
314 of 2,5-diketopiperazines (DKPs) such as cyclo(Pro-Val), cyclo(Leu-Pro), cyclo(Pro-
315 Pro) and cyclo(Pro-pyroGlu), as pyrolytic markers, although assignment to a given
316 protein fiber, e.g. wool or silk, was impossible because no specific pyrolytic markers
317 have been identified so far (Orsini et al., 2017).

318 The pyrogram of a typical PP particle as identified by FTIR, namely the blue fiber S3.2,
319 is shown in Figure 3.a, while the corresponding main detected pyrolysis products are
320 reported in Table S-4 in the SD. The intense peak from 2,4-dimethyl-1-heptene is a

321 characteristic marker of PP (Dierkes et al., 2019); such assignment is confirmed by the
322 presence of the typical clusters of peaks consisting of three signals from 1,n-diene, 1-
323 alkene, and n-methyl-1,n-diene of a given PP oligomer (Castelvetto et al., 2021).

324 The pyrolytic profile of the yellow fiber S11.8 (Table S-4 in the SD), shown in Figure
325 3.b, features many signals from unsaturated nitriles such as 2,4-dicyano-1-butene (2-
326 methylenepentadinitrile) along with one from 2-methylene-pentadinitrile, both markers
327 for PAN acrylic fibers (Castelvetto et al., 2021). A very similar pyrogram was recorded
328 for the green fiber S11.9 (Figure 3.b).

329 Pyrolysis of the MPs identified by FTIR as PET led to a broad range of fragments
330 (Fig.3.c) dominated by aromatic species, such as phenylacetaldehyde, 4-methyl-benzoic
331 acid, 4-ethylbenzoic acid, 4-vinyloxy carbonyl benzoic acid, divinyl terephthalate and, in
332 particular, divinyl benzoate, in agreement with the literature (Wu et al., 2014; Dayana et
333 al., 2016). Phenyl radicals are also generated, leading to the formation of diphenyl and
334 its derivatives (Table S-4).

335 *SEM analysis*

336 Most of the ten sampled microplastic fibers and fragments selected for Scanning
337 Electron Microscopy (SEM) observation of their surface morphology were analyzed
338 without additional purification after the procedural flotation and mild oxidation
339 treatment described in the Section 2.3. Additional treatment to remove residual soiling
340 matter was only performed for the fragments 2 and 7; for this purpose they were placed
341 in a test tube with 3 mL deionized water, and mildly sonicated in a water bath for 15
342 min at 40 °C. The SEM images revealed significant differences in surface roughness in
343 both kinds (fragments and fibers) of the ten particles, indicative of different extent of
344 degradation and/or of different weathering behavior of different polymer types (Table
345 S-1 in the SD). In particular, fragments seemed to be more heavily oxidized compared to
346 fibers, showing scratches, fractures and crevices, pits and pores, protrusions and
347 grooves, in addition to some residual particles soiling their surface (Fig.4). On the other
348 hand, fibers exhibited partially damaged texture with irregular filaments and fibrillated
349 structures at the ends. In addition, some fibers also showed erosion features, with small
350 pits and cracks visible even at low magnification. Samples 2 and 7 were observed
351 before and after the mild sonication, to evaluate possible damage caused to the polymer
352 surface by the cleaning procedure. Indeed, in Fig.4 (a, b and e) the surfaces appear

353 visibly eroded as a result of the sonication performed on oxidized particles with an
354 already damaged surface. By comparing these morphological features before and after
355 sonication, SEM images revealed that the PP and PE fragments showed stronger surface
356 degradation than the PP and PE fibers. The apparently better resistance of the PE and
357 PP fibers as highlighted by their less degraded surface morphology is possibly the result
358 of shorter exposure to the environment and/or of a higher crystallinity of the fibers. It is
359 worth pointing out that a damaged surfaces with fringed and sharp edges in MPs may
360 pose a higher risk of internal injuries for the soil fauna as they travel through the
361 gastrointestinal tract (Touil et al., 2020). Finally, the numerous pits and pores observed
362 by SEM on the surface of the MPs could act as shelter for colonization by
363 microorganism communities, further impacting the MPs properties (Chai et al., 2020).

364 *3.4. Heavy metals associated with MPs*

365 Heavy metals were analyzed in both MPs and their corresponding soils at each sampling
366 site; the results are reported in Fig.5. The average concentrations of the heavy metals
367 Hg, Ti, As, Al, Fe, Zn, Mn, Cu, Cr, and Ni associated with the MPs were 40.56, 28.47,
368 21.17, 1.88, 1.19, 0.09, 0.01, 0.01, 0.009, and 0.004 $\mu\text{g}\cdot\text{g}^{-1}$, respectively. These
369 concentrations are lower than those measured on the corresponding soil matrices that
370 contained the same sequence as above at concentration 11938.75, 160.81, 31.62, 7.6,
371 7.41, 7.22, 5.20, and 7.03 $\mu\text{g}\cdot\text{g}^{-1}$, respectively.

372 The highest concentrations of heavy metals adsorbed on the MPs were those of Hg,
373 ranging from 4.27-80.58 $\mu\text{g}/\text{g}$, followed by As, up to 44.54 $\mu\text{g}/\text{g}$, and Ti, from 0.68 to
374 82.65 $\mu\text{g}/\text{g}$, lower concentrations having been found for Cr, Cu, Ni, and Mn, while the
375 concentrations of Ag, Cd and Co were below the detection threshold. The content of
376 trace metals in the soils was greater than that in the MPs, in agreement with a previous
377 study by (Zhou et al., 2019) in which the specific surface area of the soil particle,
378 comparatively larger than that of the MPs, was assumed as the main reason for the
379 former to be more effective adsorbers of pollutants (including heavy metal ions) from
380 the environment (e.g. polluted surface waters).

381 The relatively high concentrations of some less naturally common toxic metals found in
382 this study are closely associated with human activities (uncontrolled dumping, industrial
383 and household wastes) suggesting that the presence of most of them be the result of

384 adsorption from polluted agricultural soil and/or surface waters, although contributions
385 from bulk contaminants in the original plastic formulation could not be excluded.

386 The results from both laboratory experiments (Turner and Holmes, 2015) and analyses
387 on environmental soil samples e.g. (Wang et al., 2016) actually suggest that MPs are
388 potential carriers of metals from even a lightly polluted aqueous environment. Metals
389 may in this case accumulate onto the MPs surface, with increasing efficiency as the
390 particle size becomes smaller and thus the specific surface area increases. Soiling
391 material (clay, silt, etc., as well as adhered organic matter) could also contribute to the
392 accumulation of metals onto MPs by modifying their surface properties and effective
393 surface area.

394 **4. Conclusions**

395 The results of this study, aiming at assessing the state of contamination by MPs in the
396 farmland soil of Moknine province in Tunisia, showed significant pollution mostly
397 related to the local intensive agricultural practices, and in particular to extensive use of
398 plastics mulches and greenhouse coverage. The concentration of MPs in the greenhouse
399 farms was higher than in enclosed farms away from, suggesting a possible risk of
400 agricultural activities on the side of the greenhouse. The MPs isolated from soil samples
401 were identified by a combination of FTIR and Py-GC/MS. Polymer identifications by
402 Py-GC/MS and FTIR analyses on the same particle were generally in agreement
403 confirming their reliability as complementary techniques for MPs identification in
404 agricultural soil; better accuracy can obviously be achieved when both techniques are
405 applied.

406 The presence of MPs from textiles and of heavy metals, as detected by ICP-MS,
407 suggested a contribution to the overall contamination by wastewaters from nearby urban
408 and industrial sites, as they are commonly used for irrigation.

409

410

411

412

413

414 **Acknowledgements**

415 K. Chouchene acknowledges the University of Sfax for providing financial support for her
 416 internship at the University of Pisa in Italy. Scanning Electron Microscopy with FEI QUANTA
 417 450 ESEM-FEG and Py-GC/MS analyses with Frontier EGA/Py-3030D Multi-Shot Pyrolyzer
 418 plus Agilent 8890 Gas Chromatograph were performed at the Center for Instrument Sharing of
 419 the University of Pisa (CISUP).

420

421 **References**

- 422 Afrin, S., Uddin, K., Rahman, M.M., 2020. Heliyon Microplastics contamination in the
 423 soil from Urban Land fi ll site , 6. <https://doi.org/10.1016/j.heliyon.2020.e05572>
- 424 Castelvetro, V., Corti, A., Nasa, J. La, Modugno, F., Ceccarini, A., Giannarelli, S.,
 425 Vinciguerra, V., Bertoldo, M., 2021. Polymer Identification and Specific Analysis
 426 (PISA) of Microplastic Total Mass in Sediments of the Protected Marine Area of
 427 the Meloria Shoals 13, 1–18.
 428 <https://doi.org/https://doi.org/10.3390/polym13050796>
- 429 Chai, B., Wei, Q., She, Y., Lu, G., Dang, Z., Yin, H., 2020. Soil microplastic pollution
 430 in an e-waste dismantling zone of China. *Waste Manag.* 118, 291–301.
 431 <https://doi.org/10.1016/j.wasman.2020.08.048>
- 432 Chairi, R., Derenne, S., Abdeljaoued, S., Largeau, C., 2010. Sediment cores representative of
 433 contrasting environments in salt flats of the Moknine continental sabkha (Eastern
 434 Tunisia): Sedimentology, bulk features of organic matter, alkane sources and
 435 alteration. *Organic Geochemistry* 41, 637–652.
 436 <https://doi.org/10.1016/j.orggeochem.2010.04.006>
- 437 Chen, Y., Leng, Y., Liu, X., Wang, J., 2019. Microplastic pollution in vegetable
 438 farmlands of suburb Wuhan, central China. *Environ. Pollut.* 113449.
 439 <https://doi.org/10.1016/j.envpol.2019.113449>
- 440 Chouchene, K., Pinto, J., Wali, A., Girão, A. V., Hentati, O., Duarte, A.C., Rocha-
 441 santos, T., Ksibi, M., 2019. Microplastic pollution in the sediments of Sidi
 442 Mansour Harbor in Southeast Tunisia. *Mar. Pollut. Bull.* 146, 92–99.
 443 <https://doi.org/10.1016/j.marpolbul.2019.06.004>
- 444 Chouchene, K., Rocha-santos, T., Ksibi, M., 2020. Selected case studies on the
 445 environment of the mediterranean and surrounding, occurrence , and distribution of
 446 microplastics and metals contamination in sediments from south west of
 447 Kerkennah archipelago , Tunisia. [https://doi.org/https://doi.org/10.1007/s11356-](https://doi.org/https://doi.org/10.1007/s11356-020-09938-z)
 448 [020-09938-z](https://doi.org/https://doi.org/10.1007/s11356-020-09938-z)
- 449 Corradini, F., Meza, P., Eguiluz, R., Casado, F., Huerta-lwanga, E., Geissen, V., 2019.
 450 Science of the Total Environment Evidence of microplastic accumulation in
 451 agricultural soils from sewage sludge disposal. *Sci. Total Environ.* 671, 411–420.
 452 <https://doi.org/10.1016/j.scitotenv.2019.03.368>
- 453 Dayana, S., Sharuddin, A., Abnisa, F., Mohd, W., Wan, A., 2016. A review on pyrolysis
 454 of plastic wastes. *Energy Convers. Manag.* 115, 308–326.

- 455 <https://doi.org/10.1016/j.enconman.2016.02.037>
- 456 Dierkes, G., Lauschke, T., Becher, S., Schumacher, H., Földi, C., Ternes, T., 2019.
457 Quantification of microplastics in environmental samples via pressurized liquid
458 extraction and pyrolysis-gas chromatography.
459 <https://doi.org/https://doi.org/10.1007/s00216-019-02066-9>
- 460 Ding, L., Zhang, S., Wang, X., Yang, X., Zhang, C., Qi, Y., Guo, X., 2020. Science of the
461 Total Environment The occurrence and distribution characteristics of
462 microplastics in the agricultural soils of Shaanxi Province , in north-western China.
463 *Sci. Total Environ.* 720, 137525. <https://doi.org/10.1016/j.scitotenv.2020.137525>
- 464 Galafassi, S., Nizzetto, L., Volta, P., 2019. Science of the Total Environment Plastic
465 sources : A survey across scientific and grey literature for their inventory and
466 relative contribution to microplastics pollution in natural environments , with an
467 emphasis on surface water. *Sci. Total Environ.* 693, 133499.
468 <https://doi.org/10.1016/j.scitotenv.2019.07.305>
- 469 Li, D., Zhou, L., Wang, X., He, L., Yang, X., 2019. Effect of Crystallinity of
470 Polyethylene with Different Densities on Breakdown Strength and Conductance
471 Property. <https://doi.org/https://doi.org/10.3390/ma12111746>
- 472 Liu, M., Lu, S., Song, Y., Lei, L., Hu, J., Lv, W., Zhou, W., Cao, C., Shi, H., Yang, X.,
473 He, D., 2018. Microplastic and mesoplastic pollution in farmland soils in suburbs
474 of Shanghai,China. *Environ. Pollut.* <https://doi.org/10.1016/j.envpol.2018.07.051>
- 475 Lv, Weiwei, Zhou, W., Lu, S., Huang, W., Yuan, Q., Tian, M., Lv, Weiguang, He, D.,
476 2019. Science of the Total Environment Microplastic pollution in rice- fish co-
477 culture system : A report of three farmland stations in Shanghai , China. *Sci. Total*
478 *Environ.* 652, 1209–1218. <https://doi.org/10.1016/j.scitotenv.2018.10.321>
- 479 Lwanga, E.H., Gertsen, H., Gooren, H., Peters, P., Ploeg, M. Van Der, Besseling, E.,
480 Koelmans, A.A., Geissen, V., 2016. Microplastics in the Terrestrial Ecosystem :
481 Implications for *Lumbricus*. <https://doi.org/10.1021/acs.est.5b05478>
- 482 Majewsky, M., Bitter, H., Eiche, E., Horn, H., 2016. Science of the Total Environment
483 Determination of microplastic polyethylene (PE) and polypropylene (PP) in
484 environmental samples using thermal analysis (TGA-DSC). *Sci. Total Environ.*
485 568, 507–511. <https://doi.org/10.1016/j.scitotenv.2016.06.017>
- 486 Nizzetto, L., Langaas, S., Futter, M., 2016. Pollution: Do microplastics spill on to farm
487 soils? *Nature* 537, 488. <https://doi.org/10.1038/537488b>
- 488 Orsini, S., Parlanti, F., Bonaduce, I., 2017. *Journal of Analytical and Applied Pyrolysis*
489 Analytical pyrolysis of proteins in samples from artistic and archaeological objects.
490 *J. Anal. Appl. Pyrolysis* 124, 643–657. <https://doi.org/10.1016/j.jaap.2016.12.017>
- 491 Pinto, J., 2018. ScienceDirect Micro- and nanoplastics in the environment : Research
492 and policymaking. *Curr. Opin. Environ. Sci. Heal.* 1, 12–16.
493 <https://doi.org/10.1016/j.coesh.2017.11.002>
- 494 Primpke, S., Fischer, M., Lorenz, C., Gerds, G., Scholz-Böttcher, B., 2020.
495 Comparison of pyrolysis gas chromatography / mass spectrometry and
496 hyperspectral FTIR imaging spectroscopy for the analysis of microplastics.
497 <https://doi.org/https://doi.org/10.1007/s00216-020-02979-w>

- 498 Samir, S., Elsamahy, T., Koutra, E., Kornaros, M., El-sheekh, M., Abdelkarim, E.A.,
499 Zhu, D., Sun, J., 2021. Science of the Total Environment Degradation of
500 conventional plastic wastes in the environment : A review on current status of
501 knowledge and future perspectives of disposal. *Sci. Total Environ.* 771, 144719.
502 <https://doi.org/10.1016/j.scitotenv.2020.144719>
- 503 Scheurer, M., Bigalke, M., 2018. Microplastics in Swiss Floodplain Soils.
504 <https://doi.org/10.1021/acs.est.7b06003>
- 505 Steinmetz, Z., Wollmann, C., Schaefer, M., Buchmann, C., David, J., Tröger, J., Muñoz,
506 K., Frör, O., Ellen, G., 2016. Science of the Total Environment Plastic mulching in
507 agriculture . Trading short-term agronomic benefits for long-term soil
508 degradation ? *Sci. Total Environ.* 550, 690–705.
509 <https://doi.org/10.1016/j.scitotenv.2016.01.153>
- 510 Touil, S., Nacer, M., Omira, C., 2020. Impact assessment of long treated wastewater
511 irrigation on soil and crops in Algeria. *Euro-Mediterranean J. Environ. Integr.* 7, 1–
512 10. <https://doi.org/10.1007/s41207-020-00187-7>
- 513 Turner, A., Holmes, L.A., 2015. Adsorption of trace metals by microplastic pellets in
514 fresh water. <https://doi.org/https://doi.org/10.1071/EN14143>
- 515 Van Sebille, E., Wilcox, C., Lebreton, L., Maximenko, N., Hardesty, B.D., Van
516 Franeker, J.A., Eriksen, M., Siegel, D., Galgani, F., Law, K.L., 2015. A global
517 inventory of small floating plastic debris. *Environ. Res. Lett.* 10, 124006.
518 <https://doi.org/10.1088/1748-9326/10/12/124006>
- 519 Wali, A., Kawachi, A., Seddik, M., Bougi, M., 2015. Effects of Metal Pollution on
520 Sediments in a Highly Saline Aquatic Ecosystem : Case of the Moknine
521 Continental Sebkh (Eastern Tunisia). <https://doi.org/10.1007/s00128-015-1469-9>
- 522 Wang, Xiaoning, Bi, W., Zhai, P., Wang, Xiaobing, Li, H., Mailhot, G., Dong, W.,
523 2016. Applied Surface Science Adsorption and photocatalytic degradation of
524 pharmaceuticals by BiOCl_x / Y nanospheres in aqueous solution. *Appl. Surf. Sci.*
525 360, 240–251. <https://doi.org/10.1016/j.apsusc.2015.10.229>
- 526 Wu, T., Hu, H.L., Du, Y.P., Jiang, D., Yu, B.H., 2014. International Journal of Polymer
527 Analysis and Characterization Discrimination of Thermoplastic Polyesters by
528 MALDI-TOF MS and Py-GC / Discrimination of Thermoplastic Polyesters by
529 MALDI-TOF MS and Py-GC = MS 37–41.
530 <https://doi.org/10.1080/1023666X.2014.920126>
- 531 Zhou, Q., Zhang, H., Fu, C., Zhou, Y., Dai, Z., Li, Y., 2018. Geoderma The distribution
532 and morphology of microplastics in coastal soils adjacent to the Bohai Sea and the
533 Yellow Sea. *Geoderma* 0–1. <https://doi.org/10.1016/j.geoderma.2018.02.015>
- 534 Zhou, Y., Liu, X., Wang, J., 2019. Science of the Total Environment Characterization of
535 microplastics and the association of heavy metals with microplastics in suburban
536 soil of central China. *Sci. Total Environ.* 694, 133798.
537 <https://doi.org/10.1016/j.scitotenv.2019.133798>
- 538 Zhu, B., Fang, Y., Zhu, D., Christie, P., Ke, X., Zhu, Y., 2018. Exposure to nanoplastics
539 disturbs the gut microbiome in the soil oligochaete *Enchytraeus crypticus* *.
540 *Environ. Pollut.* 239, 408–415. <https://doi.org/10.1016/j.envpol.2018.04.017>

541

542

Journal Pre-proof

543 **Figure captions**

544

545 **Figure.1:** Sampling location in Moknine area, and the sixteen sampling points of agriculture
546 soils.

547 **Figure.2:** Microscopic images of observed fibers detected in the agricultural soils by A, B, C,
548 D: Dark field and A1, B1, C1, D1 UV light of PP and PAN.

549

550 **Figure.3:** Chromatogram Pyrolysis-GC/MS of (A): PP (Blue, Grey and White fiber), (B): PAN
551 (Green fiber) and (C): PET (Grey fiber).

552 **Figure.4:** SEM images of the surface morphology of some microplastic particles; A (S2), B
553 (S1) and E(S7) (Sonicated): surface of PE fragment., C (S12) and D (S4): PP fibers surface
554 and F(S13): the surface of Nylon fiber.

555 **Figure.5:** Heavy metal contents in MPs and in the corresponding soils ($\mu\text{g}\cdot\text{g}^{-1}$) of each
556 sampling site.

557

558 **Supplementary material**

559 **Figure.S-1:** The polymer: (A): types, (B): size and (C): colors distribution of MPs within
560 sixteen samples from the region of Moknine province.

561

562 **Figure.S-2:** Chemical identification of MPs polymers via FTIR; *A: HDPE: high-density*
563 *Polyethylene; B: LDPE: low-density Polyethylene or LLDPE: Linear low-density*
564 *Polyethylene; C: PP: Polypropylene; D: PAN: Polyacrylonitrile E: Nylon; F: PET:*
565 *Polyester; G: cellulose.*

566 **Figure.S-3:** Differential scanning calorimetry thermal of two polyethylene fragments.

567

568 **Table.S-1:** Observation of the morphology of microplastics by SEM: interpretation of the sign
569 degradation referred to figure legend.

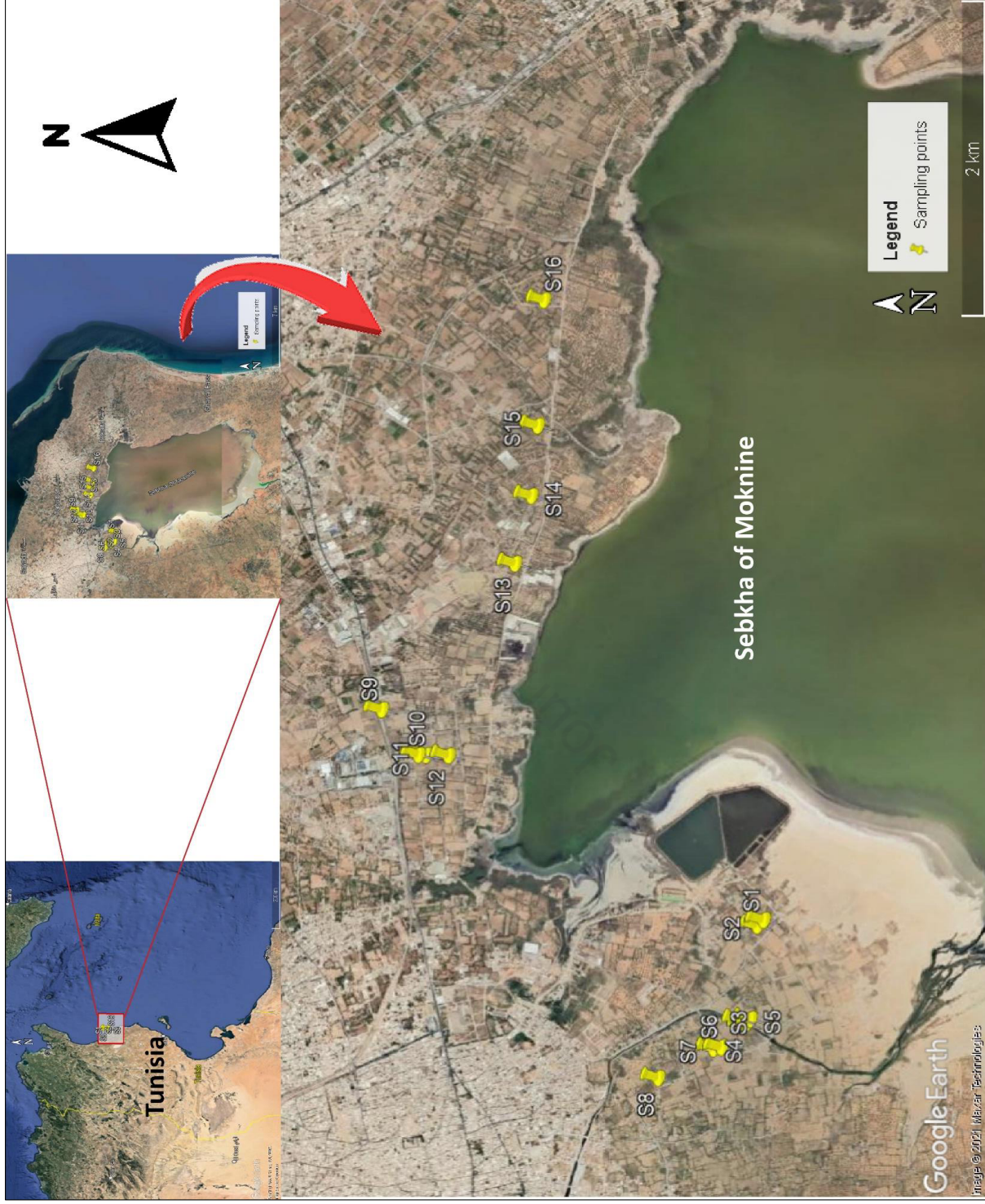
570 **Table.S-2:** Important absorption bands and assignment for -FTIR spectra of MPs detected in the
571 agriculture soils.

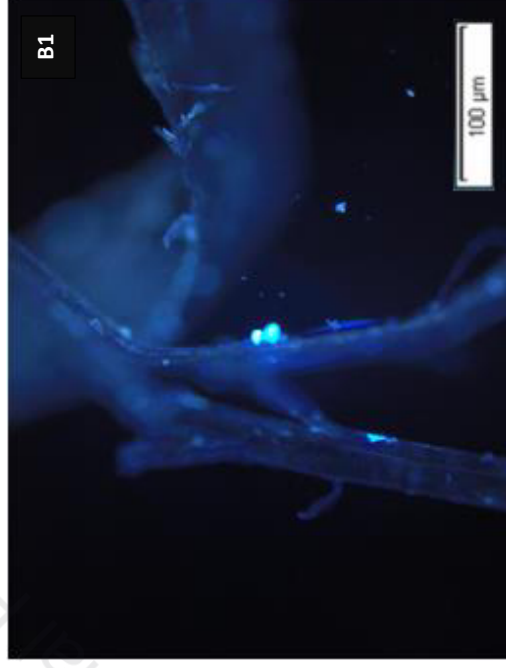
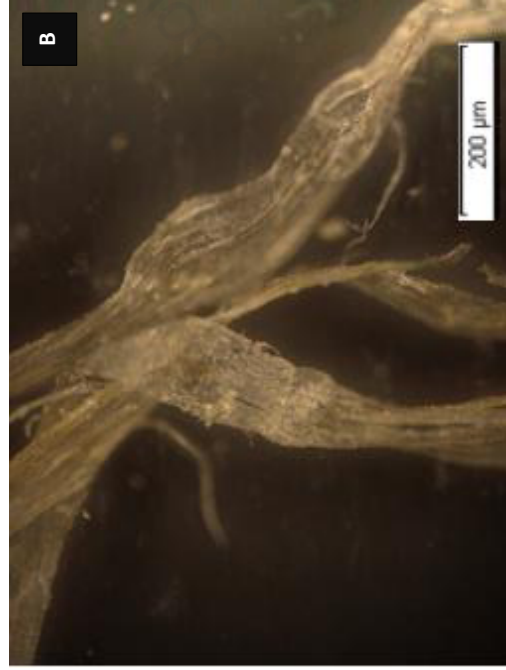
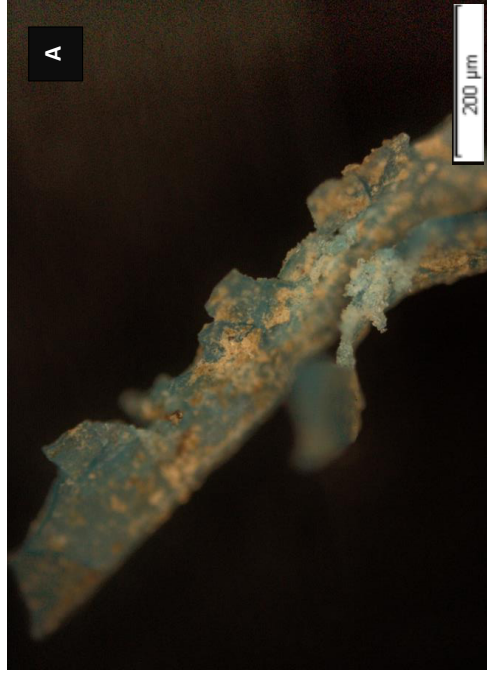
572 **Table.S-3:** Main Pyrolysis product of different fiber microplastics.

573 **Table.S-4:** Application of pyrolysis coupled to gas chromatography and mass spectrometry (Py-
574 GC/MS) to the characterization of fibers in environmental samples, in the context of the
575 study of MPs contamination in agricultural soil in Moknine, Tunisia.

576

577





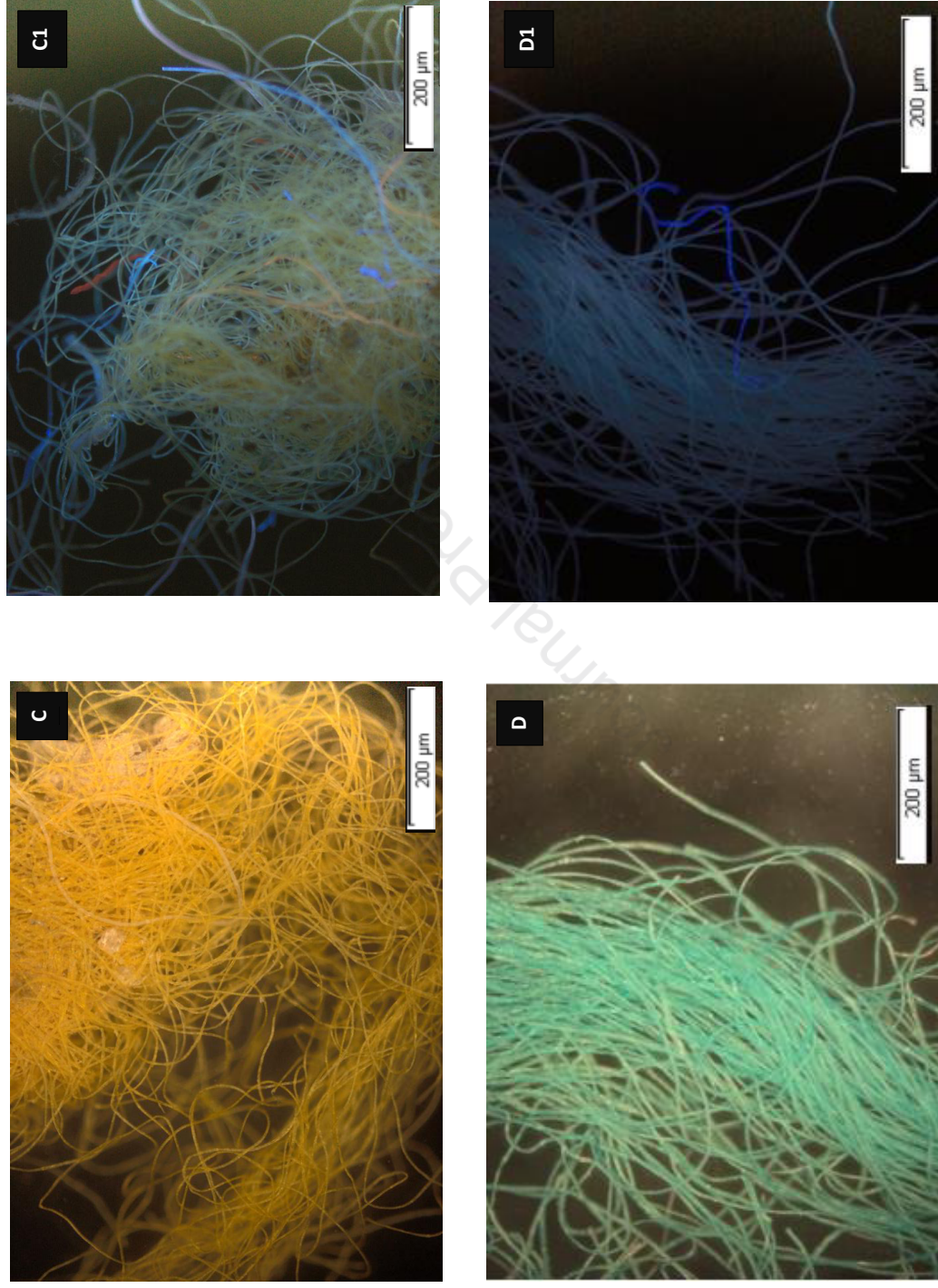
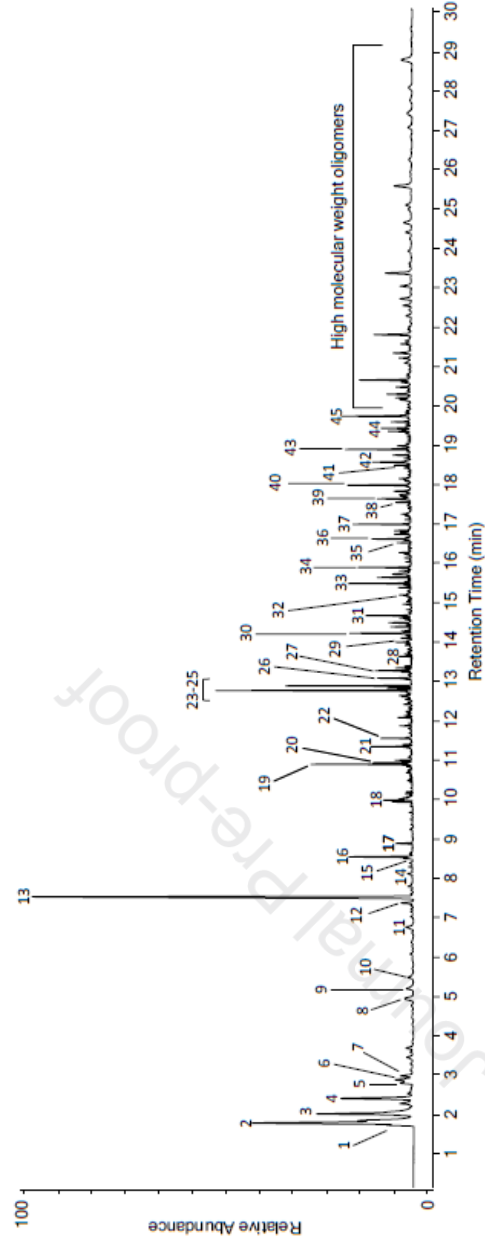
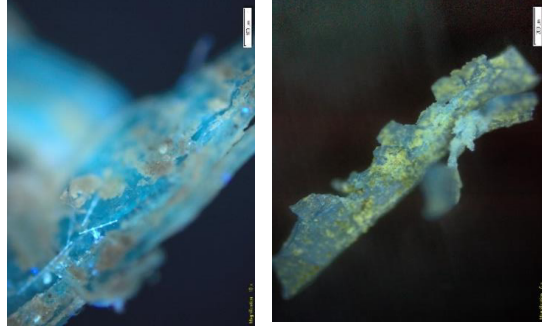


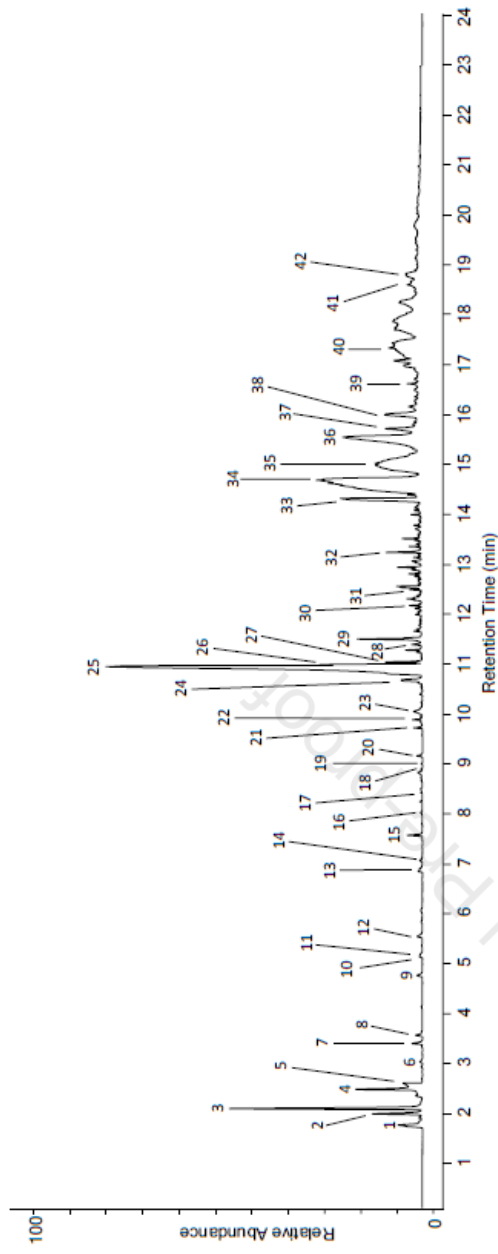
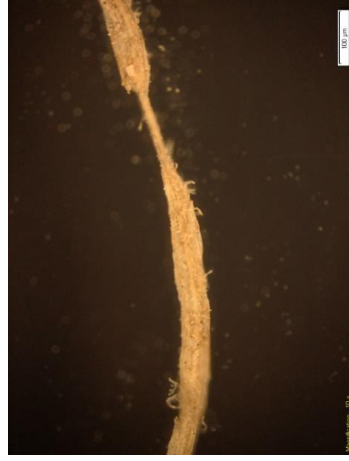
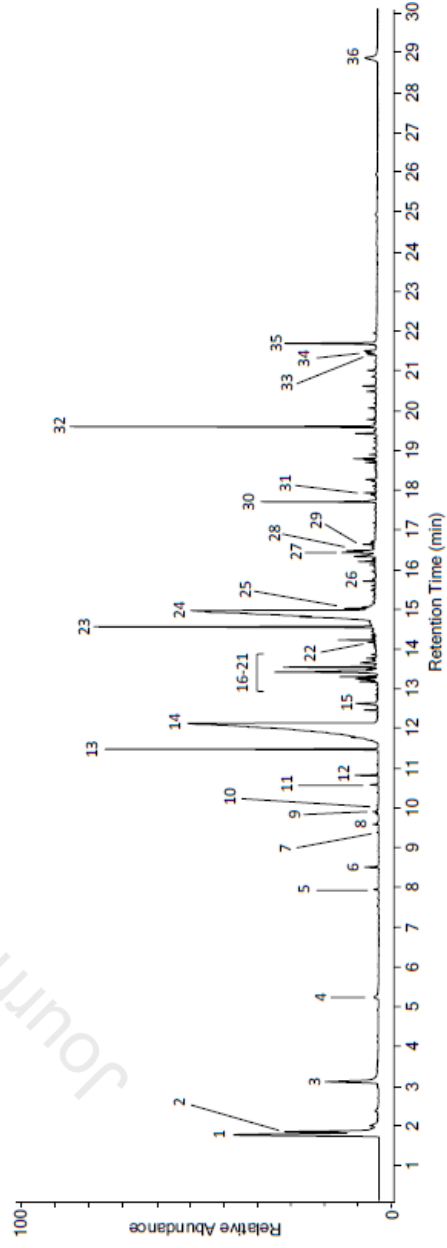
Figure.2

Journal Pre-proof

Journal Pre-proof

A: Py-GC-MS pyrogram of PP fibers (Blue, Grey and White fiber)



B: Pyrolysis-GC-MS of PAN (Green fiber)**C: Pyrolysis-GC-MS of PET (Grey fiber)****Figure.3**

Journal Pre-proof

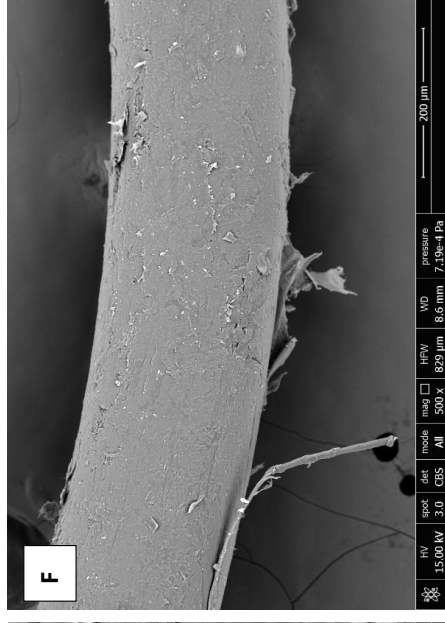
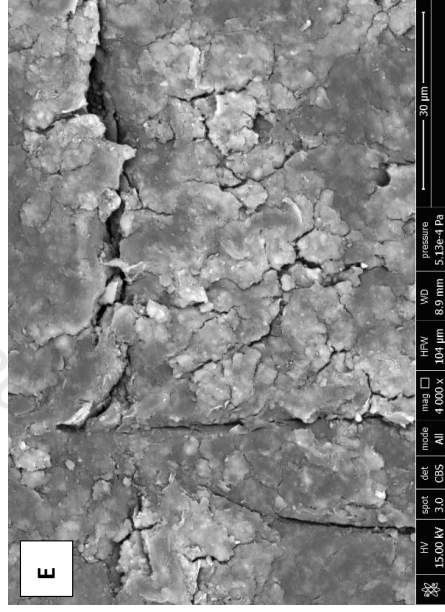
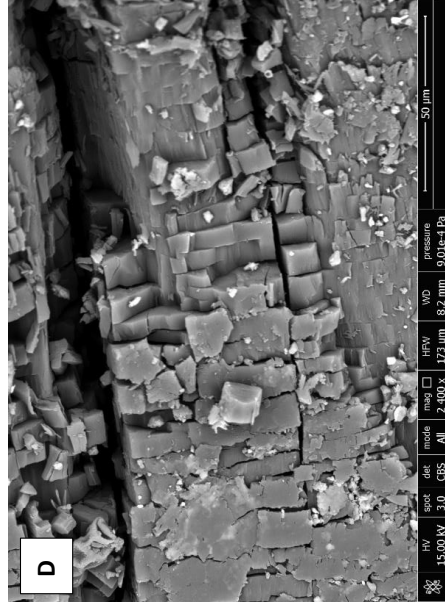
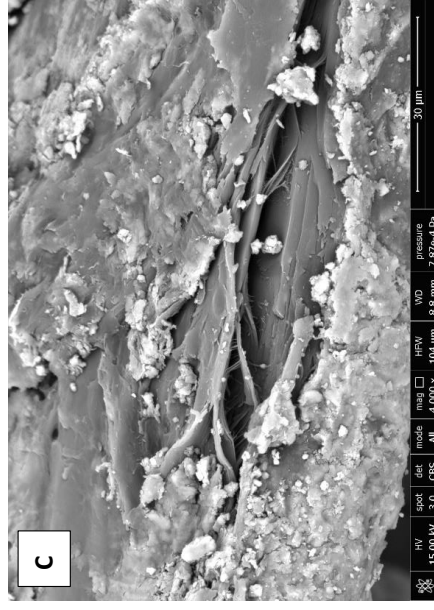
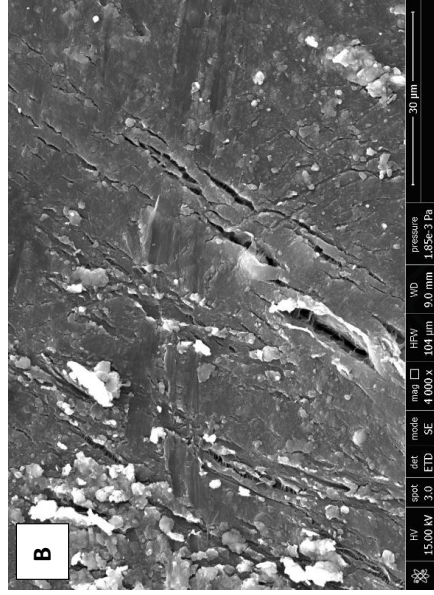
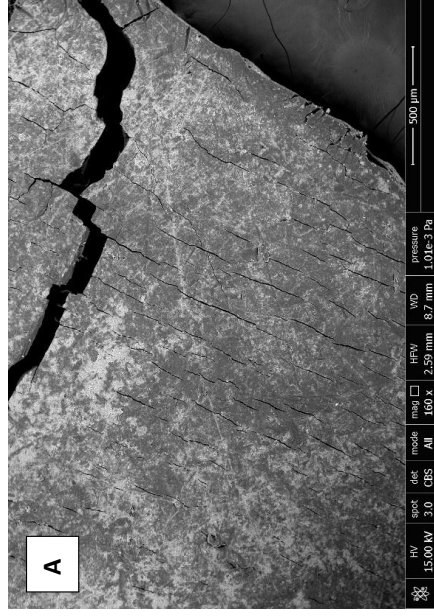
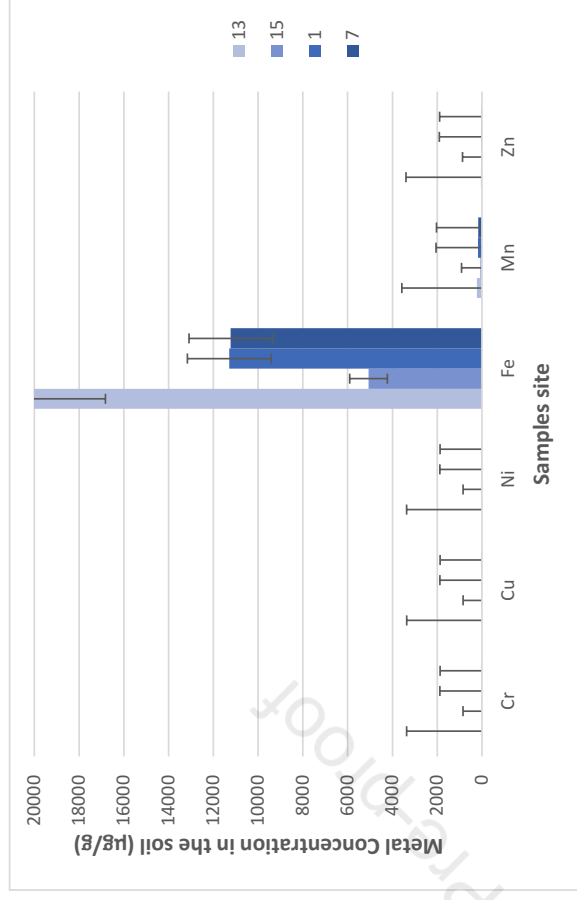
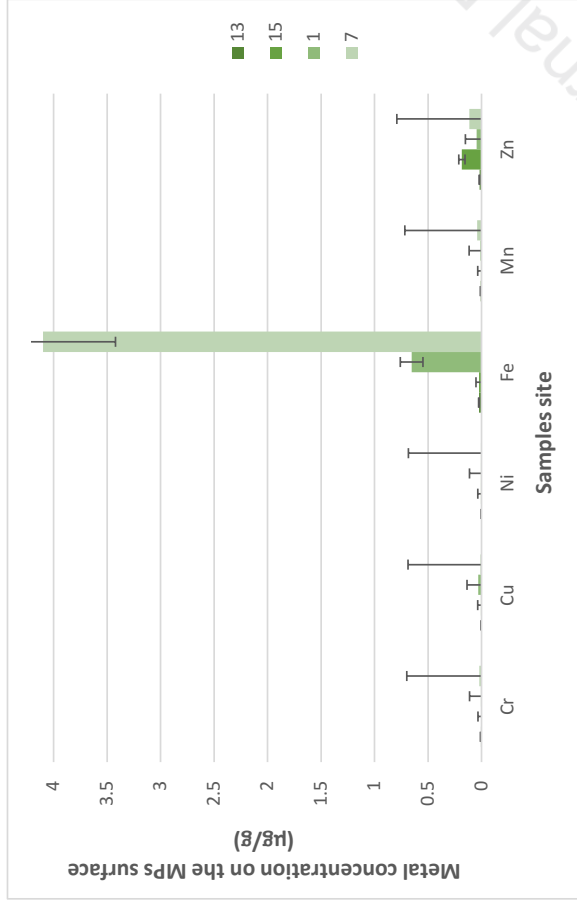


Figure.4: SEM images of the surface morphology of some microplastic particles; A (S2), B (S1) and E(S7) (Sonicated): surface of PE fragment., C (S12) and D (S4): PP fibers surface and F(S13): the surface of Nylon fiber.

Journal Pre-proof



A B

Figure.5: Heavy metal contents in MPs and in the corresponding soils ($\mu\text{g}\cdot\text{g}^{-1}$) of each sampling site.

Journal Pre-proof

- Microplastics (MPs) were isolated from intensive farming soils of Tunisia
- The concentration of MPs in the soils investigated ranged from 50 to 880 items/kg
- Synthetic textile fibers shorter than 1 mm were the dominant MPs types
- The greenhouse and plastic mulch have been identified as possible MPs point source.
- DSC and Py-GC/MS technique offer a promising option in the field of MPs analysis

Journal Pre-proof

AUTHORSHIP STATEMENT

Manuscript title: Soil contamination by microplastics in relation to local agricultural development as revealed by FTIR, ICP-MS and pyrolysis-GC/MS

All persons who meet authorship criteria are listed as authors, and all authors certify that they have participated sufficiently in the work to take public responsibility for the content, including participation in the concept, design, analysis, writing, or revision of the manuscript. Furthermore, each author certifies that this material or similar material has not been and will not be submitted to or published in any other publication before its appearance in *the journal of Environmental Pollution*.

Authorship contributions

Please indicate the specific contributions made by each author (list the authors' initials followed by their surnames, e.g., Y.L. Cheung). The name of each author must appear at least once in each of the three categories below.

Category 1

Conception and design of study: k. Chouchene, M. Ksibi , , ;
 acquisition of data: K. Chouchene , T. Nacci , , ;
 analysis and/or interpretation of data: k. Chouchene, M. Ksibi , , , .

Category 2

Drafting the manuscript: K. Chouchene , M. Ksibi , , ;
 revising the manuscript critically for important intellectual content: V. Castelvetro , F. Modugno ,
 T. Nacci , .

Category 3

Approval of the version of the manuscript to be published (the names of all authors must be listed):
 K. Chouchene , T. Nacci , F. Modugno , V. Castelvetro , M. Ksibi ,
 , ,

Acknowledgements

All persons who have made substantial contributions to the work reported in the manuscript (e.g., technical help, writing and editing assistance, general support), but who do not meet the criteria for authorship, are named in the Acknowledgements and have given us their written permission to be named. If we have not included an Acknowledgements, then that indicates that we have not received substantial contributions from non-authors.

Declaration of interests

The authors declare that they have no known competing financial interests or personal relationships that could have appeared to influence the work reported in this paper.

The authors declare the following financial interests/personal relationships which may be considered as potential competing interests:

Journal Pre-proof